# Liquid−Vapor Interfaces of Simple Electrolyte Solutions: Molecular Dynamics Results for Ions in Stockmayer Fluids

**Sandip Paul and Amalendu Chandra***

*Department of Chemistry, Indian Institute of Technology, Kanpur, India 208016*

*Received: February 28, 2003; In Final Form: August 26, 2003*

The equilibrium and dynamical properties of liquid−vapor interfaces of electrolyte solutions are investigated by employing a simple model where the ions are represented by charged Lennard-Jones particles and the dipolar solvent molecules are characterized by the so-called Stockmayer potential. The technique of molecular dynamics simulation is employed to calculate the density profiles and the orientational structure of the interfaces, the surface tension, the translational and rotational diffusion coefficients, and also the dipole orientational relaxation times of both interfacial and bulk molecules. It is found that the ions prefer to stay in the interior of the solutions and tend to avoid the surfaces. The dipole vectors of the interfacial solvent molecules tend to align parallel to the surfaces. The surface tension shows an increasing trend with increase of ion concentration, and this increase of the surface tension is found to be the net outcome of a decrease of the solvent−solvent contribution and an increase of the ion−solvent and ion−ion contributions. The dynamical properties of the interfaces are found to be different from those of the corresponding bulk liquid phases. The solvent molecules at the interfaces rotate and translate in the parallel direction at a faster rate than that of bulk molecules. The perpendicular diffusion, however, occurs at a slower rate for the interfacial molecules. Also, on increase of ion concentration of the solutions, the dynamical properties of the interfaces are found to change differently from those of the bulk solutions. The equilibrium and dynamical results of the present interfacial solutions are also compared with the results of liquid−vapor interfaces of aqueous NaCl solutions that were reported in an earlier study (*Chem. Phys. Lett.* **2003**, *373*, 87).

## 1. Introduction

The molecular aspects of liquid−vapor interfaces of ionic solutions have been a topic of current interest both experimentally and theoretically. The experimental studies of these systems have primarily employed the nonlinear optical techniques,[1−4] whereas the majority of the recent theoretical studies have involved the technique of molecular dynamics simulations.[5−11] Although the analytical theoretical studies of liquid−vapor interfaces of ionic solutions started long ago,[12−14] none of the existing theories deal with such interfaces at the molecular level. The so-called primitive model has been the standard model for analytical theoretical studies of liquid−vapor interfaces of electrolyte solutions where molecular solvent is replaced by a structureless dielectric continuum.[12−17] This is in contrast to the situation with pure dipolar solvents, for which rather detailed molecular theories of liquid−vapor interfaces are available in the literature.[18−22]

The existing computer simulation studies of the liquid−vapor interfaces of ionic solutions deal with aqueous solutions where the molecularity of water is taken into account explicitly.[5−11] The water molecules are modeled by multisite interaction potentials so that its hydrogen bond network structure at molecular level is properly accounted for. The aqueous solutions are rather complex systems because of their hydrogen bond network. The modification of this hydrogen bond network at surfaces plays a role in influencing the interfacial properties of such systems. Besides, for aqueous ionic solutions, the situation is further complicated by the formation of hydrogen bonds between anions and hydrogens of water molecules and also by the asymmetric solvation of cations and anions by water molecules. Because of this complexity of the existing simulation systems, in the present work we have aimed at studying a simple model as a reference system for liquid−vapor interfaces of ionic solutions and investigate their equilibrium and dynamical properties at a molecular level. From theoretical point of view, liquid−vapor interfaces of the solutions of nonpolarizable spherical ions in Stockmayer liquids appear to be simple model systems for learning about the interfacial properties of electrolyte solutions. Because the present model is simple and may also be tractable theoretically, the present simulation results can serve as benchmarks with which the results of future molecular theories, as opposed to current continuum theories, of liquid−vapor interfaces of electrolyte solutions can be compared. This simple model of spherical ions in a Stockmayer liquid has already been employed in both simulation and theoretical studies of ionic solutions in bulk phases[23−26] but is yet to be used for studying the properties of ionic solutions at liquid−vapor interfaces.

In this work, we have carried out detailed molecular dynamics simulations of the liquid−vapor interfaces of solutions consisting of ions in Stockmayer solvents of four different concentrations ranging from 0 M (pure solvent) to about 4.0 M, where M is the molarity of a solution. The molecular structure of the interfaces is investigated by calculating the spatial and orientational density profiles of ions and solvent molecules. The intrinsic thickness of the interfaces and the surface tension of the solutions are also calculated for varying ion concentration.

* To whom correspondence should be addressed. E-mail: amalen@iitk.ac.in.

10.1021/jp0302820 CCC: $25.00 
Published on Web 11/13/2003

Various contributions to the total surface tension such as ion−ion, ion−solvent and solvent−solvent contributions are calculated to obtain a better insight into the variation of surface tension with ion concentration. The dynamics of the interfaces are investigated in terms of the relaxation of translational and angular velocity correlation functions, anisotropic diffusion, and the dipole orientational relaxation of interfacial molecules. All these dynamical quantities are calculated as functions of the ion concentration of the bulk solutions.

The outline of the rest of the paper is as follows: In Section 2, we discuss the model and details of the present simulations, including the construction of the interfaces. In Section 3, we present the results of density profiles and orientational structure of the interfaces. In Section 4, we calculate the surface tension along with its decomposition into various contributions and, in Section 5, we discuss the various dynamical properties of the interfacial and bulk liquid regions that we have calculated in the present study. A summary of the main results and our concluding remarks are presented in Section 6.

## 2. The Model and Simulation Details

We have carried out molecular dynamics simulations of four different systems consisting of spherical ions immersed in nonpolarizable dipolar solvents. Each solvent molecule is characterized by a point dipole of magnitude ($\mu$), each positive ion has a charge ($+q$), and each negative ion a charge ($-q$). The total configurational energy of the system can be expressed in the form

$$U = {}^1/_2 \sum_{i\neq j} u_{LJ}(r_{ij}) + {}^1/_2 \sum_{i\neq j} q_i q_j / r_{ij} - \sum_i \mu_i \cdot E_i^{(q)} - {}^1/_2 \sum_i \mu_i \cdot E_i^{(\mu)} \quad (1)$$

where $E_i^{(q)}$ and $E_i^{(\mu)}$ are the electric fields at particle $i$ due to all other charges and dipoles, respectively. $u_{LJ}(r_{ij})$ is the spherically symmetric short-range Lennard−Jones interaction potential given by

$$u_{LJ}(r_{ij}) = 4\epsilon_{LJ}((\sigma_{ij}/r_{ij})^{12} - (\sigma_{ij}/r_{ij})^6) \quad (2)$$

where $\sigma_{ij} = (\sigma_i + \sigma_j)/2$, where $\sigma_i$ is the Lennard-Jones diameter of particle $i$ and $\epsilon_{LJ}$ is the well-depth parameter. In the present work, we have assumed the same values of the Lennard−Jones parameters for all the species, and hereafter, we will denote $\sigma_i$ by $\sigma$. We also assume that all particles have the same mass ($m$).

The systems studied here can be completely defined by specifying the number of ions and solvent molecules, the size of the simulation box, and the following reduced parameters: $\mu^* = (\mu^2/\epsilon_{LJ}\sigma^3)^{1/2}$, $q^* = (q^2/\epsilon_{LJ}\sigma)^{1/2}$, $T^* = k_BT/\epsilon_{LJ}$ and $I^* = I/m\sigma^2$, where $k_BT$ is the Boltzmann constant times the absolute temperature, and $I$ is the moment of inertia of a solvent molecule. For all the systems considered here, the values of the reduced parameters characterizing the solvent and ions are: $\mu^* = 1.75$, $q^* = 8.0$, and $I^* = 0.025$. The reduced temperature of all the solutions is 1.20. We note that the values of the dipole moment and the ionic charges are essentially the same as those used earlier in simulations of bulk electrolyte solutions.[24,25]

Throughout this paper, we will denote the positive ions as species 1, negative ions as species 2 and the solvent molecules as species 3. For each system, we first carried out a bulk simulation in a cubic box of $N = 864$ molecules including solvent and ions, periodically replicated in all three dimensions. The number of positive and negative ions ($N_{1,2}$) and the solvent molecules ($N_3$) are specified in Table 1 for all the systems studied here. The ionic concentration of a system is specified by the mole-fraction of the salt $X = (N_1 + N_2)/N$, the values of which are also included in Table 1. We note that, for $\sigma = 2.8$ Å, systems 2, 3, and 4 are approximately 2 M, 3 M, and 4 M solutions. For each system, after the bulk solution was properly equilibrated, two empty boxes of equal size were added on either side of the original simulation box along the $z$-dimension, and this larger rectangular box was taken as the simulation box in the next phase of the simulation run. That means the simulation cell was chosen to be of dimension $L \times L \times L_z$ with $L_z = 3L$ and the system was reequilibrated by imposing periodic boundary conditions in all three dimensions. This resulted in a lamella of approximate width $L$ separated by vacuum layers of approximate width $2L$. Some of the solvent molecules were found to vaporize to the empty space to form liquid−vapor interfaces on both sides of the lamella. For all the systems studied here, we have taken $L = 10.483\sigma$ and $L_z = 31.449\sigma$. We calculated the short-range Lennard-Jones interactions by using a spherical cutoff at distance $L/2$ and the long-range electrostatic interactions were treated by using the three-dimensional Ewald method.[27] We employed the quaternion formulation of the equations of rotational motion,[27] and for the integration over time, we adapted the leapfrog algorithm with a reduced time step $\Delta t^* = \Delta t(\epsilon_{LJ}/m\sigma^2)^{1/2} = 0.0025$. MD runs of 300 000 steps were used to equilibrate each system in the bulk phase, and then MD runs of 400 000 steps were used to equilibrate each of the liquid−vapor interfacial systems in rectangular boxes. During the equilibration, the temperature of the simulation system was kept at $T^* = 1.2$ through rescaling of the velocities. The simulations of the interfacial systems were then continued in microcanonical ensemble for another 600 000 steps for the calculation of various structural and dynamical quantities of the interfaces.

**TABLE 1: The Mole Fraction of the Salt, Number of Positive and Negative Ions ($N_{1,2}$), and of Solvent Molecules ($N_3$), with the Lengths of the Simulation Box Along $x$, $y$ ($L$) and $z$ ($L_z$) Directions and the Intrinsic Thickness of the Liquid−Vapor Interfaces ($d_{lv}$) for the Four Systems Studied in this Work**

| system | mole fract of salt | $N_{1,2}$ | $N_3$ | $L/\sigma$ | $L_z/\sigma$ | $d_{lv}/\sigma$ |
|---|---|---|---|---|---|---|
| 1 | 0.0 | 0 | 864 | 10.483 | 31.449 | 2.15 |
| 2 | 0.036 | 30 | 804 | 10.483 | 31.449 | 1.84 |
| 3 | 0.054 | 44 | 776 | 10.483 | 31.449 | 1.73 |
| 4 | 0.072 | 58 | 748 | 10.483 | 31.449 | 1.58 |

## 3. Structure of the Interfaces

We have examined the number density of the ions and the dipolar molecules and also the orientational structure of dipolar molecules both in the bulk and interfacial regions. The number densities are calculated by computing the average number of molecules or ions of a given species in slabs of thickness $\Delta z = 0.02\sigma$, lying on either sides of the central plane at $z = 0$. The effects of the anisotropic environment of the interfaces on the orientational structure of dipolar molecules are determined by calculating the orientational correlation function $\alpha^{(l)}(z)$ defined by

$$\rho_3(z,\theta) = \sum_l \alpha^{(l)}(z) P_l(\cos\theta) \quad (3)$$

where $\theta$ is the angle that a dipole vector makes with the surface normal (i.e., with the $z$-axis), $\rho_3(z,\theta)$ is the position and

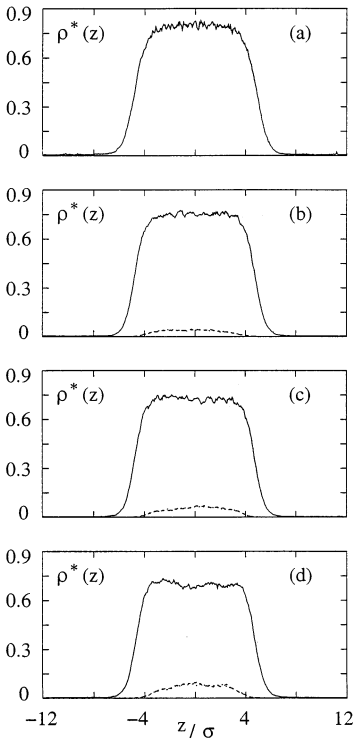


**Figure 1.** The number density of solvent molecules (solid), positive (dotted), and negative (dashed) ions in the bulk regions and at interfaces. The mole-fraction of the salt is: (a) $X = 0.0$, (b) $X = 0.036$, (c) $X = 0.054$, and (d) $X = 0.072$.

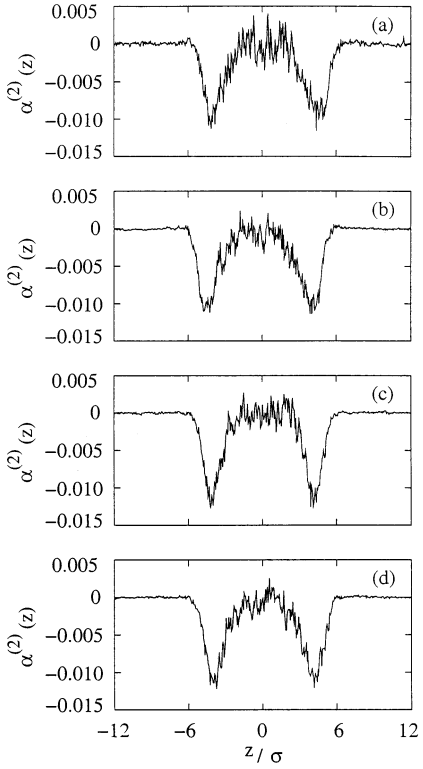


**Figure 2.** The second-rank orientational distribution function of the solvent molecules in the bulk and interfacial regions. The plots (a)−(d) are as in Figure 1

orientation dependent solvent density, and $P_l(\cos\theta)$ is the Legendre polynomial of order $l$. Clearly, orientation averaged number density of the solvent $\rho_3(z)$ is equal to $4\pi\alpha^{(0)}(z)$. Further, the symmetry of the system geometry and of the positive and negative ions ensure that there is no net polarization at the interfaces, which means $\alpha^{(1)}(z) = 0$. Thus, the most important orientational term is $\alpha^{(2)}(z)$. We note that a positive value of $\alpha^{(2)}(z)$ implies that molecules prefer to align perpendicular to the surface, and it is negative when the preferred alignment is parallel to the surface.

In Figure 1, we have shown the number densities $\rho_i(z)$ for $i = 1-3$ as a function of distance, so that the entire bulk and interfacial regions are covered. The results are shown for all the solutions of varying ion concentration. It is found that the ions prefer to remain in the interior of the solutions. Even the outermost ions are found to be about one molecular diameter below the surfaces, which means that the ions always maintain their solvation shells and so do not like to be exposed on the surfaces. Following previous work,[28] we define the intrinsic thickness ($d_{lv}$) of a liquid−vapor interface as the distance over which the number density decreases from 90 to 10% of the bulk liquid density. The values of $d_{lv}$ for the present simulation systems are also included in Table 1. It is seen that the thickness of the interfaces decreases with increase of ion concentration. This decrease of interfacial width can be attributed to the presence of ions in the liquid region which exert attractive forces on the interfacial solvent molecules, and is consistent with an increase of surface tension that is discussed in the next section. We, however, note that the thickness of the liquid−vapor interfaces of the present model solutions appears to be somewhat wider than that of the liquid−vapor interfaces of aqueous NaCl solutions studied earlier.[11] For example, for about 2M NaCl solution, the thickness $d_{lv}$ was found to be 3.05 Å $\sim 1.08\sigma$ ($\sigma \sim 2.8$ Å for water), which can be compared with the value of 1.84 found for the 2M solution of ions in Stockmayer solvent considered in the present study. We also note in this context the recent work of Jungwrith et al.,[8,9] who have shown that bromide and iodide ions, because of their rather large polarizability, prefer to stay near the surfaces rather than in the interior of the aqueous solutions. The fluoride ions were found to stay in the interior because they are essentially nonpolarizable, and the chloride ions, being of intermediate nature in terms of polarizability, were found to stay both in the interior and at the surfaces of the aqueous solutions. The cations were always found to prefer the interior regions because of their very small polarizability. Because both the cations and anions are considered to be nonpolarizable in the present study, the results of this study would be more relevant to solutions with nonpolarizable or weakly polarizable anions such as flouride or chloride ions rather than the highly polarizable larger anions.

In Figure 2, we have shown the results of the orientational profile $\alpha_2(z)$ of the dipolar molecules for all the solutions. $\alpha^{(2)}(z)$ is found to be essentially zero on the bulk regions of all the solutions, as expected. However, the values of $\alpha^{(2)}(z)$ are found to be negative in the interfacial region for all the systems, which implies that the interfacial dipolar molecules are preferentially aligned parallel to the surfaces. The extent of this parallel orientation of solvent dipoles at interfaces can be better described by calculating the probability distribution $P(\cos\theta)$ of those molecules which are found only in the interfacial region, and the results of this distribution are shown in Figure 3. In this figure, we have also included the similar results of the orientational distribution of water molecules at liquid−vapor interfaces of aqueous NaCl solutions.[11] The orientational distribution of interfacial solvent molecules is found to be rather wider for the present model solutions than that of aqueous NaCl solutions. Thus, although the parallel alignment is preferred at the interfaces, other orientations are also possible. The degree of this orientational alignment remains practically unchanged over the ion concentration range studied in this work, which is

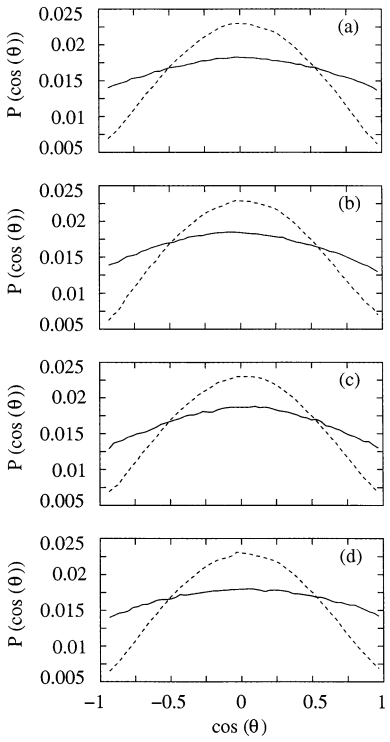


**Figure 3.** The probability function of the orientation of dipole vectors of Stockmayer solvent molecules in the interfacial region (solid curves), where $\theta$ is the angle between a dipole vector and the surface normal. The dashed curves show the corresponding results for the orientation of water dipoles at the liquid−vapor interface of aqueous NaCl solutions.[11] The plots (a)−(d) are as in Figure 1.

likely due to the fact that the ions mostly remain in the interior of the solutions and the surface regions mostly consist of only the dipolar solvent molecules. Clearly, the orientational environment of the interfaces is not noticeably affected by changing the bulk ion concentration for the model solutions considered here.

## 4. Surface Tension

We calculated the surface tension by using the following virial expression[19,29]

$$\gamma = {}^1/_{2A} < \left( \sum_{i<j} \left( r_{ij} - \frac{3z_{ij}^2}{r_{ij}} \right) \frac{\partial u_{ij}(r_{ij},\Omega_i,\Omega_j)}{\partial r_{ij}} \right) > \qquad (4)$$

where $u_{ij}(r_{ij},\Omega_i,\Omega_j)$ is the position and orientation dependent pair interaction between two particles of the solution, and the summation in eq 4 runs over all the particles including both solvent molecules and ions. $A$ is the total surface area, which is equal to $2L^2$, and $L$ is the box length along the $x$ and $y$ directions. We calculated the quantity within the parentheses in the above expression at each simulation step, and finally the averaging was done over the total number of MD steps that were run during the production phase of the simulation of a given system. Because the Lennard-Jones interaction between the particles is truncated at $r_c = L/2$ and earlier studies have shown that the effects of this potential truncation on the surface tension may not be negligible, we have combined the surface tension as obtained above with a calculation of the long range correction,[30] and the final results are shown in Table 2. The standard deviation of the surface tension data, which were calculated by using block averages over 100 000 MD steps, are about 6% of the average

**TABLE 2: The Reduced Surface Tension ($\gamma^* = \gamma\sigma^2/\epsilon_{LJ}$) of the Ionic Solutions for Varying Ion Concentration[a]**

| system | mole fract of salt | $\gamma^*$ | $\gamma^*_{ss}$ | $\gamma^*_{is}$ | $\gamma^*_{ii}$ |
|---|---|---|---|---|---|
| 1 | 0.0 | 1.47 | 1.47 | 0.0 | 0.0 |
| 2 | 0.036 | 1.60 | 1.16 | 0.34 | 0.10 |
| 3 | 0.054 | 1.66 | 1.11 | 0.43 | 0.12 |
| 4 | 0.072 | 1.74 | 1.075 | 0.53 | 0.135 |

*a* $\gamma^*_{ss}$, $\gamma^*_{is}$ and $\gamma^*_{ii}$ are the solvent−solvent, ion−solvent and ion−ion contributions to the total surface tension.

values reported in Table 2. The surface tension is found to increase with increase of ion concentration, which is in general agreement with experimental results.[31]

The increase of the surface tension with ion concentration has traditionally been explained in terms of an electrostatic effect of image forces. In these theories, which employ a primitive model where ions move in a dielectric continuum, it is argued that the presence of ions polarizes the liquid−vapor interface of the solutions. Because the dielectric constant of a polar solvent is usually much larger than that of air or vacuum, each ions image charge equals it in sign and magnitude. The repulsive interaction with the images would lead to a depletion of ion density at the interfaces, and according to Gibbs adsorption isotherm, this depletion of ion density near the surfaces causes an increase of the surface tension. Thus, the increase of surface tension is considered to arise from ion−ion interactions. Because in the simulations it is possible to decompose the surface tension into its various components, we have calculated the ion−ion, solvent−solvent, and ion−solvent contributions to the total surface tension to obtain a better insight into the various factors that lead to an enhancement of the surface tension. The results of these different contributions to the surface tension are shown in Table 2 for all the solutions. It is seen that, as the ion concentration is increased, the ion−ion and ion−solvent contributions increase, and the solvent−solvent contribution decreases. The increase of the ion−ion contribution is, however, much smaller compared to the increase of ion−solvent contribution. Also, because of the partial cancellation of the different contributions, the net increase of the surface tension with ion concentration is significantly different from any particular contribution. These results show the importance of incorporating the molecularity of the solvent in the calculations of surface tension of ionic solutions, which is missing in the present continuum-model-based theories.

## 5. Dynamics of the Interfaces

We present various dynamical properties of the solvent molecules at liquid−vapor interfaces of the electrolyte solutions that we have considered in the present work. Our goal was to study the perturbations of the solvent dynamics induced by the inhomogeneous and anisotropic environment of the interfaces. We would also like to investigate the effects of ion concentration on the dynamics of the interfaces and to compare them with those of the bulk regions. Beacause the ions are found to prefer the interior of the solutions and avoid the surfaces, we have not attempted to calculate any of the dynamical properties of the ions at the interfaces. Such results would not be statistically meaningful because of the finite simulation runs. We have calculated the velocity and angular velocity autocorrelation functions, translational and rotational diffusion coefficients, and also the relaxation of dipolar orientational correlation functions of interfacial and bulk solvent molecules. We denote the $\alpha$-th component of velocity of a dipolar molecule by $v_\alpha(t)$ ($\alpha = x, y,$

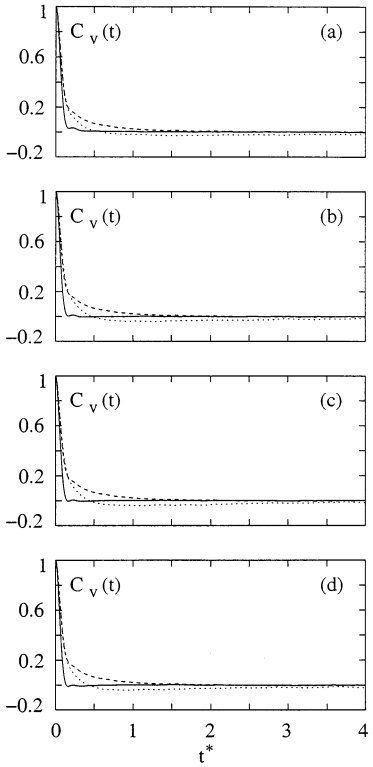


**Figure 4.** The time dependence of the *x* (dashed) and *z* (dotted) components of the velocity autocorrelation function of solvent molecules in the interfacial region for solutions of salt mole fraction: (a) $X = 0.0$, (b) $X = 0.036$, (c) $X = 0.054$, and (d) $X = 0.072$. The solid curve in each plot shows the results for bulk solvent molecules.

*z*), and its normalized velocity autocorrelation function $C_{v;\alpha}(t)$ is defined by

$$C_{v:\alpha}(t) = \frac{< v_\alpha(t) v_\alpha(0) >}{< v_\alpha(0)^2 >} \tag{5}$$

where $< \cdots >$ represents an equilibrium ensemble average. The diffusion coefficient along the α-th direction is related to the corresponding velocity-velocity autocorrelation function through the following relation

$$D_\alpha = \frac{k_B T}{m} \int_0^\infty C_{v;\alpha}(t) \mathrm{d}t \tag{6}$$

In Figure 4, we have shown the decay of the parallel (*x*) and perpendicular (*z*) components of the velocity autocorrelation functions of the interfacial dipolar molecules. In these calculations, the average of eq 5 is carried out over those molecules that are found in the interfacial region at time 0 and also at time *t*. The range of the interface is determined by the 90−10% rule as described above. The results of the velocity relaxation of bulk molecules are also shown for comparison.

It is seen that the parallel and perpendicular components of the velocity autocorrelation function of interfacial molecules decay differently due to the anisotropic environment of the interfaces. The velocity relaxation of interfacial molecules is found to occur at a slower rate than that of bulk molecules, which can be attributed to reduced collisional effects due to the lower density of the interfaces. The somewhat stronger negative regions of the perpendicular velocity autocorrelation function are manifestations of the dragging of interfacial molecules toward the liquid side, due to the higher density of the latter. This dragging would cause an inward pull and rebounce of solvent molecules from the surface region toward the liquid side, and this leads to a smaller value of the $D_z$ than $D_{x,y}$ at all concentrations, as can be seen from Table 3. The diffusion coefficients are calculated by integrating the velocity autocorrelation functions up to $t^* = 5$. When compared with the bulk dynamics, the diffusion at interfaces is found to be faster in the parallel (*x*,*y*) directions but slower in the perpendicular direction. This behavior is in contrast with liquid−vapor interfaces of aqueous NaCl solutions where the interfacial diffusion was found to be faster than that in the bulk phases for both parallel and perpendicular directions.[11] In Figure 5, we have shown the relative changes of the diffusion coefficients of interfacial and bulk molecules for varying ion concentration. In this figure, the values of the diffusion coefficients of interfacial and bulk solvent molecules are normalized by the corresponding values of the pure solvent. It is seen that, with increase of ion concentration, the parallel diffusion of the interfacial molecules shows a weaker decrease, whereas the perpendicular diffusion shows a stronger decrease compared to that of bulk molecules. It has been found that the ions prefer to stay in the interior of the solution, and thus, with increase of bulk ion concentration, the ion density in the bulk liquid region increases substantially, but the increase is much smaller in the interfacial regions. Clearly, the solvent molecules in the interfacial regions feel much less ionic friction for movement in the parallel directions than those in the bulk liquid, and as a result, the parallel diffusion coefficients of interfacial solvent molecules depend less strongly on bulk ion concentration than what is shown by the interior solvent molecules. The relatively higher ion concentration in the interior liquid region also means an enhanced dragging of the interfacial molecules toward the liquid side, and this causes a relatively stronger dependence of the perpendicular diffusion on ion concentration.

**TABLE 3: Values of the Translational and Rotational Diffusion Coefficients and the Orientational Relaxation Times in Bulk Solution (*B*) and at Interfaces (*I*)[a]**

| system | mole fract of salt | $D^*(B)$ | $D^*_{x,y}(I)$ | $D^*_z(I)$ | $\Theta^*(B)$ | $\Theta^*(I)$ | $\tau^*_\mu(B)$ | $\tau^*_\mu(I)$ |
|---|---|---|---|---|---|---|---|---|
| 1 | 0.0 | 0.090 | 0.20 | 0.023 | 2.24 | 2.60 | 0.31 | 0.30 |
| 2 | 0.036 | 0.078 | 0.19 | 0.016 | 1.76 | 2.48 | 0.50 | 0.38 |
| 3 | 0.054 | 0.073 | 0.18 | 0.012 | 1.64 | 2.37 | 0.55 | 0.42 |
| 4 | 0.072 | 0.070 | 0.17 | 0.010 | 1.56 | 2.32 | 0.58 | 0.45 |

[a] The various quantities are defined in the text. The reduced diffusion coefficients and the relaxation times are defined as: $D^* = D\sqrt{m/\epsilon_{LJ}\sigma^2}$, $\Theta^* = \Theta(m\sigma^2/\epsilon_{LJ})^{1/2}$ **and** $\tau^*_\mu = \tau_\mu/\sqrt{m\sigma^2/\epsilon_{LJ}}$.

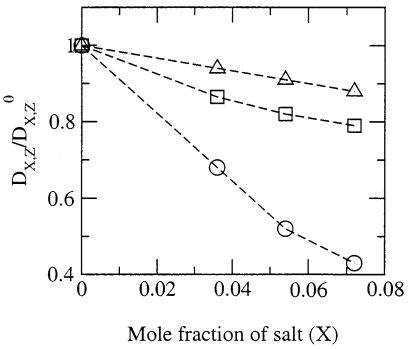


**Figure 5.** The relative changes of the diffusion coefficients of solvent molecules in the interfacial and bulk regions with increase of ion concentration of the solutions. $D^0_{x,z}$ denotes the corresponding value for the pure solvent. The triangles and the circles denote the values of parallel (*x*,*y*) and perpendicular (*z*) diffusion at interfaces and the squares represent the values of diffusion coefficients in the bulk phases. The dashed lines are drawn to guide the eye.

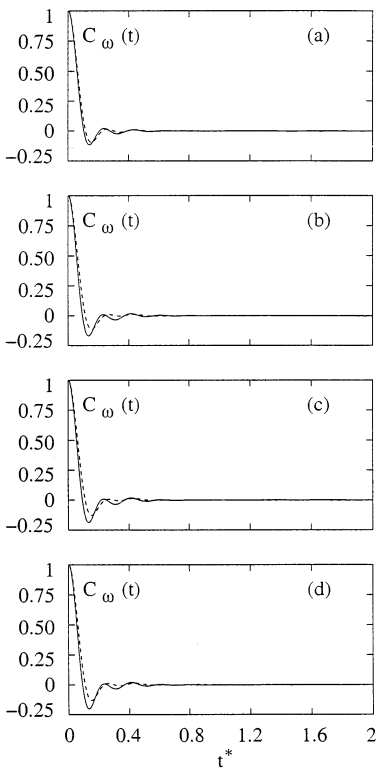


**Figure 6.** The time dependence of the angular velocity autocorrelation function of solvent molecules at interfaces (dashed) and in bulk regions (solid) for solutions of salt mole fraction: (a) $X = 0.0$, (b) $X = 0.036$, (c) $X = 0.054$, and (d) $X = 0.072$.

We next discuss the rotational dynamical properties of the interfacial solvent molecules. We define the angular velocity autocorrelation function as

$$C_\omega(t) = \frac{< \omega(t) \cdot \omega(0) >}{< \omega(0)^2 >}, \tag{7}$$

where $\omega(t)$ is the angular velocity of a solvent molecule at time $t$. The rotational diffusion coefficient $\Theta$ can be obtained from the time integral of $C_\omega(t)$ as follows

$$\Theta = \frac{k_B T}{I} \int_0^\infty \mathrm{d}t C_\omega(t) \tag{8}$$

The rotational motion of dipolar molecules can also be studied by calculating the time dependence of the self-dipole correlation function

$$C_\mu(t) = \frac{< \mu(t) \cdot \mu(0) >}{< \mu(0)^2 >} \tag{9}$$

where $\mu(t)$ is the dipole vector of a solvent molecule at time $t$. The orientational relaxation time $\tau_\mu$ is defined as the time integral of the orientational correlation function

$$\tau_\mu = \int_0^\infty C_\mu(t)\, \mathrm{d}t \tag{10}$$

As before, we have calculated the time dependence of the angular velocity and the self-dipole correlation functions of interfacial and bulk solvent molecules for all the solutions, and the results are shown in Figures 6 and 7. The values of the corresponding rotational diffusion coefficients and orientational relaxation times are included in Table 3. In the calculation of the orientational relaxation times, we have computed the integral

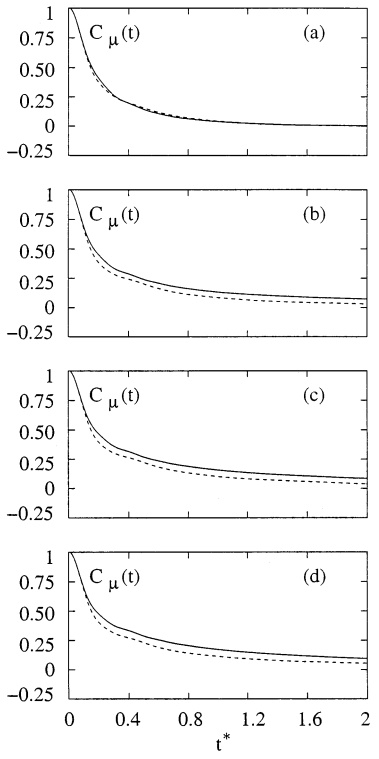


**Figure 7.** The time dependence of the dipole orientational correlation function of solvent molecules at interfaces (dashed) and in bulk regions (solid) for solutions of salt mole fraction: (a) $X = 0.0$, (b) $X = 0.036$, (c) $X = 0.054$ and (d) $X = 0.072$.

of eq 10 explicitly up to $t^* = 4$ by using the simulation data of $C_\mu(t)$, and the contribution of the tail part is obtained by using the fitted exponential functions.

In general, the relaxation of $C_\omega(t)$ for interfacial molecules is found to be somewhat slower than that of bulk molecules, due to the reduced density of the interfaces. However, the difference is rather small compared to that for the translational motion. With increase of ion concentration, the bulk relaxation shows enhanced caging and faster dynamics due to the presence of ions that tend to increase the friction that acts on the rotational motion of the dipolar molecules. Similar effects are also seen in the relaxation of the self-dipole correlation functions, which show a faster decay for interfacial molecules indicating a reduced friction on the rotation of solvent dipoles at the interfaces compared to that in the bulk phases. The results of $\Theta$ and $\tau_\mu$ show a relatively small difference between the rotational dynamics of interfacial and bulk molecules for pure water but a larger difference for the ionic solutions. In Figure 8, we have shown the variation of $\Theta$ and $\tau_\mu$ with bulk ion concentration. As in Figure 5, the values of the dynamical quantities of this figure are normalized by the corresponding values for pure solvent. With increase of ion concentration, the slowing down of the rotational motion at interfaces is found to be weaker than that in the bulk phases, which can be attributed to the ions' preference for staying in the interior of the solutions and avoiding the surfaces. A similar behavior was also found for the dynamical properties of liquid−vapor interfaces of aqueous NaCl solutions.[11] However, the relative increase of the rotational relaxation times with ion concentration and also the differences of the interfacial and bulk dynamics of the present model solutions are found to be somewhat stronger than those of aqueous NaCl solutions.[11] We note that for aqueous solutions, both the interfacial and bulk dynamics are influenced by the presence of hydrogen bonds, but no such hydrogen bonds are

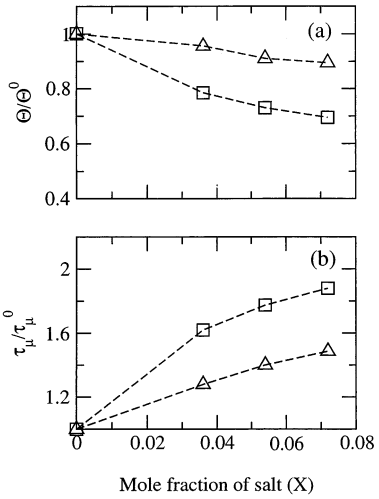


**Figure 8.** The relative changes of the (a) rotational diffusion coefficients and (b) dipole orientational relaxation times of solvent molecules in the interfacial and bulk regions with increase of ion concentration of the solutions. $\Theta^0$ and $\tau_\mu^0$ denote the corresponding values for the pure solvent. The triangles and the circles denote, respectively, the values at interfaces and in the bulk phases. The dashed lines are drawn to guide the eye.

present in the present model solutions of ions in Stockmayer solvent.

## 6. Summary and Conclusions

We have presented detailed molecular dynamics results for the structure, surface tension, and dynamical properties of liquid−vapor interfaces of simple electrolyte solutions of varying ion concentration. The ions are considered to be nonpolarizable spherical particles, which are modeled as charged Lennard-Jones spheres. The solvent molecules are also nonpolarizable and are characterized by the so-called Stockmayer potential, which consists of short-range Lennard-Jones interaction and long-range dipole−dipole interaction. This model of spherical ions in Stockmayer solvent has been used rather extensively in the studies of dynamical properties of bulk electrolyte solutions,[24−26,32] and thus, the present study can be considered as an extension of those earlier studies to inhomogeneous liquid−vapor interfaces.

It is found that the ions prefer to stay in the interior of the solutions. Even the outermost ions are found to be about one molecular diameter below the surfaces, which means the ions always prefer to be solvated and so tend to avoid the surface areas. The dipole vectors of the interfacial solvent molecules prefer to align parallel to the surfaces, although the orientational distribution is found to be rather broad. The degree of orientational alignment remains practically unchanged over the ion concentration range studied in this work. Also, the orientational order of interfacial molecules is found to be relatively weaker than that of water molecules at liquid−vapor interfaces of interfacial aqueous solutions.[11] The intrinsic width of the interfaces shows a decreasing trend, and the surface tension shows an increasing trend with increase of ion concentration. The increase of the surface tension is found to be the net outcome of a decrease of solvent−solvent contribution and an increase of ion−solvent and ion−ion contributions. This is an important result in view of the fact that all existing theories of surface tension of ionic solutions employ a continuum model of the solvent and consider only the ion−ion contribution as the factor responsible for the increase of surface tension. The present results clearly show the importance of incorporating all the contributions, and hence, the molecularity of the solvent, in the calculations of the surface tension of electrolyte solutions.

Among the dynamical properties of the interfaces, we have calculated the velocity and angular velocity autocorrelation functions, the translational and rotational diffusion coefficients and also the dipole orientational relaxation times of interfacial solvent molecules. The velocity relaxation at the interface is found to be slower than that in the bulk liquid. However, the negative region at intermediate times, which corresponds to the caging effects, is found to be somewhat stronger for the perpendicular velocity relaxation at interfaces. Accordingly, we found a faster parallel diffusion and a slower perpendicular diffusion at interfaces compared to that in the bulk liquid phases. This behavior is somewhat different from that of aqueous NaCl solutions where both the parallel and perpendicular diffusions at interfaces were found to be faster than that of bulk molecules.[11] In general, the solvent molecules at the interfaces are found to rotate at a faster rate than that of bulk molecules. Also, the orientational relaxation times of interfacial solvent molecules are found to show a weaker slowing down than those of the bulk molecules on increase of ion concentration of the solutions due to the preferential presence of the ions in the bulk liquid regions. Among the various components of the interfacial diffusion tensor, the perpendicular diffusion shows a relatively stronger dependence on ion concentration than the parallel diffusion. This is likely due to the higher density of ions in the bulk liquid region, which drags and enhances the rebounce of solvent molecules from the surfaces in the perpendicular direction. Similar behavior was also found in simulations of liquid−vapor interfaces of aqueous NaCl solutions, although the relative decrease of diffusion coefficients and increase of rotational relaxation times with increasing ion concentration as well as the relative differences of the interfacial and bulk dynamics are found to be somewhat stronger for the present simple solutions of ions in Stockmayer solvent.

In the present work, we have considered positive and negative ions of equal size, and as a result, we found an identical density profile for both the ions. It would be interesting to explore the effects of varying size of the cations and anions on their density profiles in the bulk and interfacial regions. It would also be interesting to calculate the dynamical properties of the interfaces with polarizable ions, especially when the negative ions are larger in size. We hope to address these issues in future publications.

## References and Notes

(1) Eisenthal, K. B. *Chem. Rev.* **1996**, *96*, 1343.
(2) Shultz, M. J.; Baldelli, S.; Schnitzer, C.; Simonelli, D. *J. Phys. Chem. B* **2002**, *106*, 5313.
(3) Zimdars, D.; Eisenthal, K. B. *J. Phys. Chem. B* **2001**, *105*, 3993; Benderskii, A. V.; Eisenthal, K. B. *J. Phys. Chem. B* **2001**, *105*, 6698.
(4) Schnitzer, C.; Baldelli, S.; Shultz, M. J. *J. Phys. Chem. B* **2000**, *104*, 585; Schnitzer, C.; Baldelli, S.; Campbell, D. J.; Shultz, M. J. *J. Phys. Chem. A* **1999**, *103*, 6383.
(5) Benjamin, I. *Chem. Rev.* **1996**, *96*, 1449.
(6) Wilson, M. A.; Pohorille, A.; Pratt, L. R. *Chem. Phys. Lett.* **1989**, *129*, 209.
(7) Stuart, S. J.; Berne, B. J. *J. Phys. Chem. A* **1999**, *103*, 10300.
(8) Jungwirth, P.; Tobias, D. J. *J. Phys. Chem. B* **2000**, *104*, 7702. Jungwirth, P.; Tobias, D. J. *J. Phys. Chem. B* **2001**, *105*, 10468. Jungwirth, P.; Tobias, D. J. *J. Phys. Chem. A* **2002**, *106*, 379.
(9) Jungwirth, P.; Tobias, D. J. *J. Phys. Chem. B* **2002**, *106*, 6361.
(10) Dang, L. X.; Chang, T.-M. *J. Phys. Chem. B* **2002**, *106*, 235; Dang, L. X. *J. Phys. Chem. B* **2002**, *106*, 10388.
(11) Paul, S.; Chandra, A. *Chem. Phys. Lett.* **2003**, *373*, 87.
(12) Wagner, C. *Phys. Z.* **1924**, *25*, 474.
(13) Onsager, L.; Samaras, N. N. T. *J. Chem. Phys.* **1934**, *2*, 528.
(14) Buff, F. P.; Stillinger, F. H. *J. Phys. Chem.* **1955**, *11*, 312.

(15) Weiss, V. C.; Schroder, W. *J. Phys. Condens. Matter* **2000**, *12*, 2637.
(16) Levin, Y. *J. Chem. Phys.* **2000**, *113*, 9722.
(17) Markin, V. S.; Volkov, A. G. *J. Phys. Chem. B* **2002**, *106*, 11810.
(18) Eggerbrecht, J.; Gubbins, K. E. Thompson, S. M. *J. Chem. Phys.* **1987**, *86*, 2286.
(19) Eggerbrecht, J.; Thompson, S. M.; Gubbins, K. E. *J. Chem. Phys.* **1987**, *86*, 2299.
(20) Frodl, P.; Dietrich, S. *Phys. Rev. A* **1992**, *45*, 7330. *Phys. Rev. E*, **1993**, *48*, 3741.
(21) Yang, B.; Sullivan, D. E.; Tjipto-Margo, B.; Gray, C. G. *Mol. Phys.* **1992**, *76*, 709.
(22) Yang, B.; Sullivan, D. E.; Gray, C. G. *J. Phys. Condens. Matter* **1994**, *6*, 4823.
(23) Caillol, J. M.; Levesque, D.; Weis, J. J. *J. Chem. Phys.* **1986**, *85*, 6645.
(24) Chandra, A.; Wei, D.; Patey, G. N. *J. Chem. Phys.*, **1993**, *98*, 4959. Chandra, A.; Wei, D.; Patey, G. N. *J. Chem. Phys.* **1993**, *99*, 2083.
(25) Chandra, A.; Patey, G. N. *J. Chem. Phys.* **1994**, *100*, 8385.
(26) Neria, E.; Nitzan, A.; *J. Chem. Phys.* **1994**, *100*, 3855.
(27) Allen, M. P.; Tildesley, D. J. *Computer Simulation of Liquids*; Oxford, 1987.
(28) Taylor, R. S.; Dang, L. X.; Garrett, B. C. *J. Phys. Chem.* **1996**, *100*, 11720.
(29) Kirkwood, J. G.; Buff, F. P. *J. Chem. Phys.* **1949**, *17*, 338.
(30) Mecke, M.; Winkelmann, J.; Fischer, J. *J. Chem. Phys.* **1999**, *110*, 1188.
(31) *CRC Handbook of Chemistry and Physics*, edited by R. C. Weast et al.; CRS Press: Boca Raton, Florida, **1989**.
(32) Chandra, A. *Chem. Phys. Lett.* **1995**, *244*, 314. Chandra, A. *Chem. Phys. Lett.* **1996**, *253*, 456.